

Infrared Dielectric Mirrors Based on Thin Film Multilayers of Polystyrene and Polyvinylpyrrolidone

James Bailey, James S. Sharp

School of Physics and Astronomy and Nottingham Nanotechnology and Nanoscience Centre, University of Nottingham, University Park, Nottingham, NG7 2RD, United Kingdom

Correspondence to: J. S. Sharp (E-mail: james.sharp@nottingham.ac.uk)

Received 22 December 2010; revised 17 February 2011; accepted 22 February 2011; published online 2011

DOI: 10.1002/polb.22238

ABSTRACT: Thin film polymer multilayers were prepared by spin coating alternating layers of polystyrene and polyvinylpyrrolidone. Samples with 10, 20, 30, 40, and 50 layers were prepared with individual layer thickness values in the range 223–508 nm. These samples were measured using a Fourier transform infrared spectrometer and were found to display narrow photonic band gaps (~0.04 to 0.06 μm wide) in their spectral response over the wavelength range 1.6–2.6 μm . The position of the photonic band gaps was controlled by varying the thickness of the individual layers within the multilayer structures. This was achieved by varying the spin speed used during the deposition of the polymer layers. The peak reflectance of the multilayers was controlled by varying the number of layers within the multilayer samples giving values in the range 20–80% (corresponding to transmittances of

80–20%). Calculated transmittance spectra were also obtained using an optical transfer matrix method. These calculated spectra were shown to be in good agreement with the experimental data obtained. These experiments demonstrate a facile approach to the production of low cost dielectric mirrors that have tailored photonic properties over a range of wavelengths that are currently important for applications in fibre optic based telecommunications. © 2011 Wiley Periodicals, Inc. *J Polym Sci Part B: Polym Phys* 49: 732–739, 2011

KEYWORDS: films; FT-IR; infrared spectroscopy; optics; spin coating; thin films

INTRODUCTION Dielectric mirrors have found numerous applications in the manufacture of optical filters,¹ resonant cavity LEDs,² solar cells,³ and lasers.^{4–8} These structures are manufactured by building up alternating layers of materials with different refractive indices to form a stratified multilayer structure.^{1–10} The difference in refractive index at the boundary between successive layers causes a small amount of light to be reflected at each interface. If many such layers are stacked in series, the result is an increase in the amount of light that is reflected from the structure. Interesting optical effects arise when the spatial variations in refractive index occur on length scales that are comparable to the wavelength of the incident radiation.¹⁰ Under these circumstances, such samples are observed to reflect light over a narrow range of wavelengths that are associated with the production of standing wave states inside the multilayer structure. This region of enhanced reflection corresponds to the opening of a photonic band gap within the optical response of the structure and the position of this band gap is simply controlled by varying the spatial period associated with the refractive index changes in the structure (i.e., the thickness of the individual layers).

The position/wavelength (λ_0) and width ($\Delta\lambda$) of the dominant reflection peak are determined by the individual layer

thickness values (d_1 and d_2) and the layer refractive indices (n_1 and n_2) to give¹⁰

$$\lambda_0 = 2(n_1d_1 + n_2d_2) \quad (1)$$

and

$$\Delta\lambda = \frac{4\lambda_0}{\pi} \arcsin\left(\frac{n_2 - n_1}{n_2 + n_1}\right) \quad (2)$$

Fabrication of dielectric mirrors is usually performed by using expensive ultra high vacuum (UHV) based techniques to deposit inorganic materials.¹¹ The reason for using inorganics is that it is possible to increase the optical contrast (difference in refractive index) between the layers to maximize the amount of reflection at each interface and hence reduce the total number of layers that are required to give the desired peak reflectance values.^{1–7} However, the UHV techniques that are employed to build these structures are often expensive and the precursor materials can be toxic. Another feature of inorganic dielectric mirrors is that the photonic bands that are produced can often be broad (~ a few hundred nanometres). However we note that some commercially available inorganic optical coatings are available which have narrow

high quality reflectance/photonic bands. While having broad photonic bands is an advantage for the production of broad band reflector based applications, it is a serious disadvantage for applications where narrow reflectance bands are desirable such as dichroic mirrors and acousto-optic modulators.

Polymeric materials provide a method of producing structures which display narrow reflectance bands (photonic band gaps).¹² This is because the range of refractive indices for polymers is small (typically 1.3–1.6 in the IR-visible range),¹³ and hence the amount of optical contrast that exists between transparent polymeric materials is small in comparison to those found in inorganic multilayer systems. The main disadvantage associated with these small contrast differences is that many more layers are required in the structure to give the required peak reflectance values. However, this problem is offset by the fact that polymers are relatively cheap and can be processed into multilayer structures using solvent based^{8,9} or melt processing based approaches⁷ that do not require carefully controlled environmental conditions such as UHV.

A number of attempts have been made to manufacture both polymer/inorganic⁶ and all-polymer^{7–9,14} multilayers for use as dielectric mirrors. A few researchers have studied multilayers that reflect infrared radiation,^{15,16} but much of this work has involved the production of devices that reflect visible radiation. Such structures have been successfully incorporated into optoelectronic devices^{6–8,17} and recent experiments have also indicated that polymer based multilayer structures could have potential applications in Gigahertz acousto-optic devices which are the sound based analog of the dielectric mirrors described above.¹⁸

A key requirement during the production of polymer multilayer samples is that the deposition of new layers does not disrupt previous layers in the structure. This can be a particular concern with polymers especially when spin coating from organic solvents as the solvent for one polymer will often swell or dissolve the other type of polymer being used to build up the structure. Moreover, diffusion of the solvent being used to deposit a new layer can result in swelling or dissolution of previous layers of the same type of polymer. This causes local variations in the layer thickness and can lead to cracking or the onset of swelling induced thin film instabilities in the multilayer structures. All of these phenomena lead to an overall reduction in the reflectance of the multilayer samples. Great care must therefore be taken to ensure that the deposition of each new layer does not interfere with the previous layers. This can be achieved by building the multilayers from incompatible polymers that are deposited using mutually exclusive solvents. However, the range of available materials that fit these criteria and which have the desired contrast differences to produce high reflectances are somewhat limited.^{7–9} An additional approach to solving this problem is to treat one or more of the layer types such that they reduce the rate of diffusion of solvents through the structure when new layers are being deposited. Examples of this type of approach include cross linking of the layers or swelling in a different solvent which does not dissolve any of the layers in the structure

but prevents the transport of organic solvents through the layers.

In this manuscript we describe an experimental study of thin film polystyrene (PS) and polyvinylpyrrolidone (PVP) multilayers that are produced using spin coating. These samples are shown to reflect infrared radiation over narrow bands in the 1.6–2.6 μm wavelength region. This wavelength range is extremely important for optic fibre based telecommunications.¹⁹ The position of the measured reflectance/transmittance bands in the IR spectra of the multilayer structures was tuned throughout this range by varying the thickness of the individual layers within the samples. This was achieved by varying the spin speed that was used during spin coating of the layers. During the deposition of the multilayers it was found that high quality optical structures could only be produced if each of the PVP layers was swollen using fuming hydrochloric acid (HCl) vapor. An automated spin coater was used to control the deposition of the layers and to treat each PVP layer in this way. Fourier transform InfraRed (FTIR) spectroscopy studies showed that exposure of PVP to HCl caused no permanent chemical changes in the PVP layers and that the layers are simply swollen by the vapor. The enhanced optical properties of multilayers that are treated in this way are attributed to the production of uniform layers within the structures which have sharp interfaces between them. The HCl vapor is believed to swell the PVP layers and to prevent the diffusion of organic solvents into the underlying multilayer structures.

This study builds upon our previous experiments on similar samples that were shown to reflect light in the UV-Visible region.¹² Here we describe the first application of polystyrene/polyvinylpyrrolidone multilayers in infrared dielectric mirrors and we discuss the swelling process that is vital in protecting the developing multilayers when new layers are deposited.

EXPERIMENTAL

Multilayers of commercially available PVP (average $M_w = 1,300$ kDa, BASF, Germany) and PS (Average $M_w = 192$ kDa, Sigma, UK) were spin coated on to clean glass microscope slides (75 mm \times 25 mm) from 4 wt % solutions in ethanol/acetonitrile (50/50 weight ratio) and toluene respectively using a home built automated spin coater and solution delivery system. In each case, PVP films were deposited first and samples with 10, 20, 30, 40, and 50 alternating layers of PVP and PS were deposited on to different glass substrates. Layers were typically deposited at a rate of one every minute.

Following the deposition of each PVP layer, the samples were exposed to fuming hydrochloric acid (HCl) vapor. This was done to swell the PVP layers slightly and to protect the samples during the deposition of the next PS layer. The thickness values of the individual layers in the multilayer structures were controlled by varying the spin speed used during deposition of the films. The multilayer samples were annealed under vacuum (1 mtorr) for 5 hours at 110 $^{\circ}\text{C}$ to remove residual solvent and stresses that may have been introduced into the multilayers

during the spin coating procedure. They were then allowed to cool to room temperature before being inspected using an Olympus BX51 optical microscope. Inspection revealed that all the multilayer samples were uniform in color over large areas of the samples and contained few defects. The uniformity of the colors observed on these samples is indicative of uniform layer thickness values over the majority of the surface of the samples. However, close to the edge of the samples (within 1–2 mm of the edge of the substrate) some color variations were observed where the thickness of the samples varies due to boundary effects. These observations are consistent with those made on single films of PS and PVP that were spin coated on to similar glass substrates.

Following inspection, the infrared transmission properties of the samples were measured at normal incidence using a Digilab FTS4000 Fourier transform infrared (FTIR) spectrometer. Despite the fact that both PS and PVP are transparent materials over the range of wavelengths studied (1.6–2.6 μm), the periodic changes of the refractive index in the multilayer samples caused them to preferentially reflect certain wavelengths of light in the IR region (see Figure 1). An increase in reflectance is manifested as a reduction in Transmittance in the plots shown in Figure 1 because for a non absorbing sample $\text{Transmittance} = 1 - \text{Reflectance}$. IR measurements of glass, PVP and PS layers of different thickness values confirmed that no absorption occurred in these materials over the 1.6–2.6 μm wavelength range. However at wavelengths above 2.6 μm , both PS and PVP have vibrational absorption bands.

The refractive index of the layer materials and the glass substrate were obtained by extrapolating values obtained in the visible/near IR region to the range of wavelengths studied here.¹² Calculations of the refractive index values showed that these were approximately constant for the PVP, PS and glass over the 1.6–2.6 μm wavelength range such that $n_{\text{PVP}} = 1.51 \pm 0.01$, $n_{\text{PS}} = 1.57 \pm 0.01$ and $n_{\text{glass}} = 1.43 \pm 0.01$. These values were found to be consistent with the range of literature values obtained for PS, PVP, and glass.¹³ The thickness of the polymer layers was determined by spin coating solutions of the same polymers on to single crystal Silicon wafers using identical deposition parameters to those used during the manufacture of the multilayers. These samples were then annealed and their thickness was determined using a home built self-nulling ellipsometer (wavelength, $\lambda = 633 \text{ nm}$). Thickness values were found to lie in the ranges 336–508 nm for PVP and 223–330 nm for PS. Typical values of the uncertainty in the measured film thickness values were found to be $\pm 5 \text{ nm}$.

The root-mean square (rms) roughness of the multilayer samples was also measured using an Asylum Research MFP-3D atomic force microscope (AFM) operating in tapping mode. AFM scans were collected at several positions on the surface of each of the multilayer samples using scan sizes of $40 \mu\text{m} \times 40 \mu\text{m}$. The AFM measurements showed no evidence of defects or large scale in-plane structure on the samples other than that caused by the natural r.m.s roughness associated with spin coating. Measurements of the r.m.s surface roughness for the multilayer samples were determined to lie in

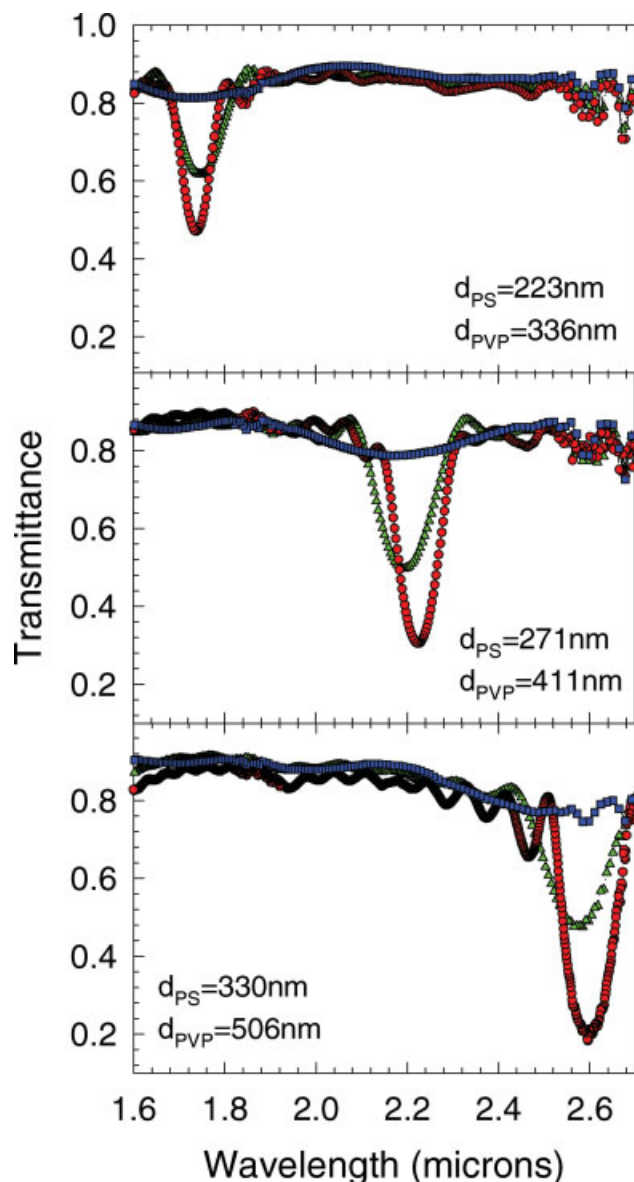


FIGURE 1 Normal incidence IR transmittance spectra for PS/PVP multilayer samples with 10 (blue \square), 30 (green \triangle), and 50 (red \circ) layers that are supported on glass substrates. Data are shown for samples where the PS and PVP film thickness values are $d_{\text{PS}} = 223 \text{ nm}/d_{\text{PVP}} = 336 \text{ nm}$ (top panel), $d_{\text{PS}} = 271 \text{ nm}/d_{\text{PVP}} = 411 \text{ nm}$ (middle panel), and $d_{\text{PS}} = 330 \text{ nm}/d_{\text{PVP}} = 506 \text{ nm}$ (top panel).

the range $1.2 \pm 0.4 \text{ nm}$ to $4.1 \pm 0.3 \text{ nm}$. The increases in roughness observed from sample to sample was consistent with an increase in individual layer thickness within the samples and is similar to that obtained from single spin cast polymer films. The low measured roughness values demonstrate that the surfaces of the samples are flat on optical length scales. This observation is consistent with the presence of the uniform interference colors that were observed on these samples.

Scanning electron microscopy (SEM) images of the layered structures were also obtained using a FEI Quanta200 3D Dual beam FIB/SEM operating at an accelerating voltage of 30 kV.

Samples were prepared by scoring the multilayer samples with a sharp scalpel blade and then gently peeling the first few layers away from the sample. The samples were then exposed to osmium tetroxide vapor (OsO_4) for 1 hour before being allowed to air dry before imaging. The OsO_4 was found to stain both polymers to slightly different degrees and was used to obtain contrast between the two materials.

A transfer matrix model²⁰ was then used to model the wavelength dependence of the transmittance (T) of the polymer multilayer samples at normal incidence. These calculations used a model which assumed perfectly sharp interfaces between the layers. The only parameters used in this model were the individual layer thickness values and the refractive indices of PVP, PS, and glass.

The effects of swelling PVP in fuming HCl vapor were also studied using FTIR spectroscopy. Thick (~ 500 nm) films of PVP and PS were prepared by spin coating the polymers on to clean calcium fluoride (CaF_2) substrates. An IR spectrum was collected for the as cast film using an uncoated CaF_2 substrate as a reference. The samples were then exposed to fuming HCl for a few seconds and IR spectra were collected for 2 days while the samples were held under ambient conditions. A similar set of samples were also produced where the samples were annealed under vacuum at 110°C for 5 hours after exposure to HCl. These samples were also studied using FTIR spectroscopy.

RESULTS AND DISCUSSION

Figure 1 shows transmittance spectra (T) obtained for spin cast multilayers of PS and PVP along with the thickness values of the PS and PVP layers that were used to manufacture the samples. Each panel of this figure shows data for samples where the layer thickness values are the same but the number of the layers in the structures varies from 10 to 50. These plots clearly show that the position of the dominant peaks in the transmittance spectra can be controlled by varying the thickness of the PS and PVP layers and that the peak transmittance value for a given sample can be varied by changing the number of layers in the structure. As the number of layers/interfaces in the samples is increased, more reflections will occur in the multilayers. This has the effect of reducing the amount of light that is transmitted by the multilayers and so samples with larger numbers of layers have smaller transmittance values in the regions corresponding to the reflection peaks. Calculations based on eq 1 which use the measured film thickness values and extrapolated refractive indices give values for the position of the dominant reflection peaks of the types of multilayers studied of 1.714, 2.092, and $2.564\ \mu\text{m}$ respectively. These values compare favorably with the corresponding measured peak positions of 1.738 ± 0.001 , 2.224 ± 0.001 , and $2.596 \pm 0.001\ \mu\text{m}$. The small differences in the measured and calculated peak positions are attributed to uncertainties in the refractive index of the PS and PVP layers (that originate from the fact that values were extrapolated from UV-Vis data) and uncertainties in the measured film thickness values (± 5 nm).

Measured values of the peak widths for the three sets of multilayers studied revealed that the half widths at half maximum

(HWHM) were 0.04 ± 0.01 , 0.05 ± 0.01 , and $0.06 \pm 0.01\ \mu\text{m}$, respectively. These are in agreement with the values of 0.040, 0.052, and 0.063 that were calculated using eq 2. The level of agreement between the calculated and measured peak positions and widths is encouraging and indicates that the multilayers that are produced during spincoating are of a high quality.

A more detailed analysis of the transmittance spectra of the multilayers was performed using a transfer matrix method. This model treats each interface in the structure as a 2×2 matrix^{20,21} which relates the magnitude of the electric fields associated with the propagating light (travelling in both directions) on one side of the interface to those on the other. The elements of the interface matrix $\mathbf{M}_{i,j}$ corresponding to the interface between layers i and j are constructed using a combination of the Fresnel reflection and transmission coefficients (r_{ij} and t_{ij})

$$\mathbf{M}_{i,j} = \begin{pmatrix} \frac{1}{t_{ij}} & \frac{r_{ij}}{t_{ij}} \\ \frac{r_{ij}}{t_{ij}} & \frac{1}{t_{ij}} \end{pmatrix} \quad (3)$$

where r_{ij} and t_{ij} at normal incidence can be written in terms of the refractive indices of layers i and j (n_i and n_j)²¹

$$r_{ij} = \frac{n_j - n_i}{n_j + n_i} \quad (4)$$

and

$$t_{ij} = \frac{2n_i}{n_j + n_i}. \quad (5)$$

Similarly, transmission through the “ i th” layer is treated using a transmission matrix of the form.

$$\mathbf{T}_i = \begin{pmatrix} e^{i\beta} & 0 \\ 0 & e^{-i\beta} \end{pmatrix} \quad (6)$$

where $\beta = \frac{2\pi d_i n_i}{\lambda}$ where d_i is the thickness of the i th layer and λ is the vacuum wavelength of the radiation. The matrix describing the entire N layer structure can then be calculated by multiplying all the interface and transmission matrices together such that

$$\mathbf{M}_{\text{tot}} = \mathbf{M}_{0,1} \mathbf{T}_1 \mathbf{M}_{1,2} \mathbf{T}_2 \dots \mathbf{M}_{N-1,N} \mathbf{T}_N \mathbf{M}_{N,\text{substrate}} \quad (7)$$

The relevant matrix elements can then be extracted and used to calculate the reflection and transmission coefficients of the entire structure (r_{tot} and t_{tot} respectively). The transmittance (T) of the multilayer is then calculated using $T = t_{\text{tot}}^2 \frac{n_{\text{sub}}}{n_0}$ where n_{sub} and n_0 are the refractive indices of the substrate and ambient, respectively.¹⁹

Figure 2 shows a comparison between experimental data and the results of calculations that were obtained using the transfer matrix method for three samples with different PS and PVP thickness values. This figure shows that the shapes of the calculated spectra are in good agreement with the measured

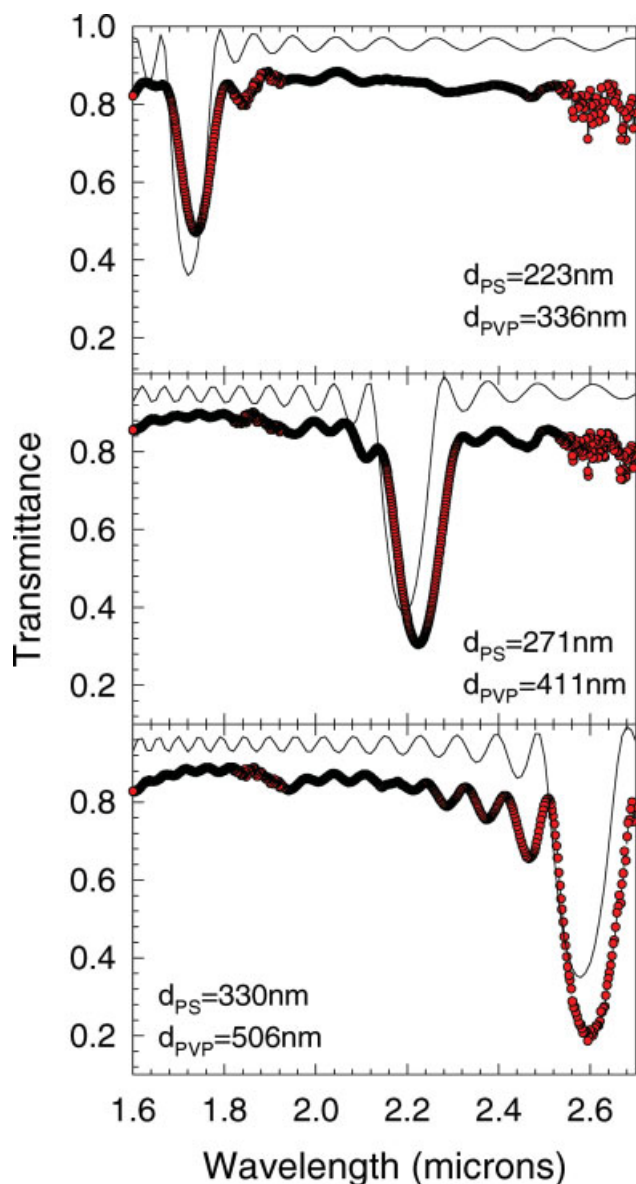


FIGURE 2 Comparison of calculated and measured transmittance spectra for PS/PVP multilayers with 50 layers. The solid lines show the results of transfer matrix calculations that were obtained using measured film thickness data and extrapolated refractive indices for the PS films, PVP films and glass substrates. The red circles are experimental transmittance data obtained from PS/PVP samples with 50 layers. Data are shown for samples where the PS and PVP film thickness values are $d_{PS} = 223$ nm/ $d_{PVP} = 336$ nm (top panel), $d_{PS} = 271$ nm/ $d_{PVP} = 411$ nm (middle panel), and $d_{PS} = 330$ nm/ $d_{PVP} = 506$ nm (top panel).

spectra. This suggests that the assumption of sharp interfaces (which is implicit in this model) provides an accurate representation of the multilayers studied here. This is to be expected given the low measured RMS roughness (~ 1 nm) of the surface of the samples and the fact that the interfacial width of spin cast polymer/polymer interfaces is expected to be tens of nanometres.²² Interfacial structure on these length scale

is expected to have a diminishing effect upon the transmission/reflection properties of polymer/polymer interfaces for wavelengths greater than ~ 1 μm . However, our previous calculations and experiments showed that interfacial structure on these length scales does influence the measured reflectance of similar samples in the UV-Visible region.¹² The inset in Figure 3 shows a SEM image of the top seven layers of a multilayer sample. These layers were extracted from the sample by scoring the multilayer, peeling off some of the layers and then staining with osmium tetroxide (OsO_4). As this image clearly shows the interfacial regions between adjacent polymer layers are very sharp (~ 10 nm wide). However, we note that the thickness of the layers in this image is not uniform. This is due to shrinkage of some of the layers during exposure to OsO_4 . The layers near the top of the sample (shown here at the bottom of the image) were exposed directly to the OsO_4 vapor, while those at the top of the image were in contact with the SEM substrate that was used to support the sample during staining. The layers in contact with the substrate were therefore expected to have less exposure to the stain used and as such will experience less shrinkage.

The positions of the baselines of the calculated spectra shown in Figure 2 are always higher than those obtained for the measured spectra. This is due to the fact that the transfer matrix calculations assume that the glass substrate supporting the multilayers is effectively infinite and therefore neglect the glass/air interface at the bottom of the substrate. The fact that the refractive index of the glass does not change significantly in the region of interest means that the change in transmittance/reflectance due to the extra glass/air interface will be approximately constant.

The top panel in Figure 3 shows the spectral response of a 40 layer multilayer sample with $d_{PS} = 271$ nm and $d_{PVP} = 411$ nm over the 1–20 μm wavelength range. The wavelength axis on this plot is scaled logarithmically so that the main regions of interest can be clearly observed. As this figure shows, the region from 1 to 3 μm contains only the reflectance bands due to the multilayer structure, but above this wavelength significant amounts of absorption are observed in the polymers (largely due to CH stretching modes²³). Above wavelengths of ~ 5 μm , the spectral response is attenuated by absorption in the substrate.

The bottom two panels in Figure 3 show a comparison of the minimum transmittance values of the dominant peaks as a function of the number of layers that were obtained from the data and calculations. The bottom panel in this figure shows a direct comparison between the data and calculations similar to those shown in Figure 2. The middle panel shows the same data with calculations where shifts due to the additional glass/air interface have been taken into account. This plot shows that there is good agreement between experiment and calculations for the multilayers with peaks at 2.224 ± 0.001 and 2.596 ± 0.001 μm , but that the data for samples with peaks at 1.738 ± 0.001 μm deviates from the calculated curves after ~ 20 layers. The reason for this is not entirely clear, but may be related to the fact that as the number of layers increases

the number of defects (e.g., dust) in the samples increases. The samples with peaks at 1.738 with more than 20 layers were generally observed to have more defects than all the other samples suggesting that great care must be taken to ensure that impurities are excluded when manufacturing these multilayer samples.

The lack of agreement between the experimental results and the predictions of the transfer matrix is also likely to arise from two other possible sources. The first source is related to

uncertainties in the film thickness values used in the calculations. As stated above, the film thickness values that were used in the calculations were obtained from measurements of single films supported on silicon substrates. There are likely to be small differences in the thickness values obtained for these films and films that are incorporated into the multilayers. This occurs for the simple reason that spin coating a polymer on top of another polymer will give a slightly different thickness value to spin coating a polymer on to a silicon substrate. The second source of uncertainty arises from the values of the refractive index of the polymer that were used in the transfer matrix calculations. As stated above, these values were obtained by extrapolating measured refractive index values from the UV-Visible region into the infrared region. While the values obtained for the refractive indices of both polymers and glass are likely to be close to the true values, they are unlikely to be exact. We therefore anticipate that there will be some deviation from the true refractive index values and this is also likely to be the reason why some of the calculated curves predict larger transmittance values than the measured data. However despite, these potential sources of uncertainty, the level of agreement between the simple model and the experimental data is encouraging.

A key factor in influencing both the physical stability of the individual layers within the multilayers and the structure of the spin cast polymer/polymer interfaces is the HCl swelling step that was applied after the deposition of each PVP layer. Tests indicate that in the absence of this swelling step the optical properties and appearance of the multilayers is degraded by the deposition of the next PS layer. However, no treatment of the multilayers is required following the deposition of each

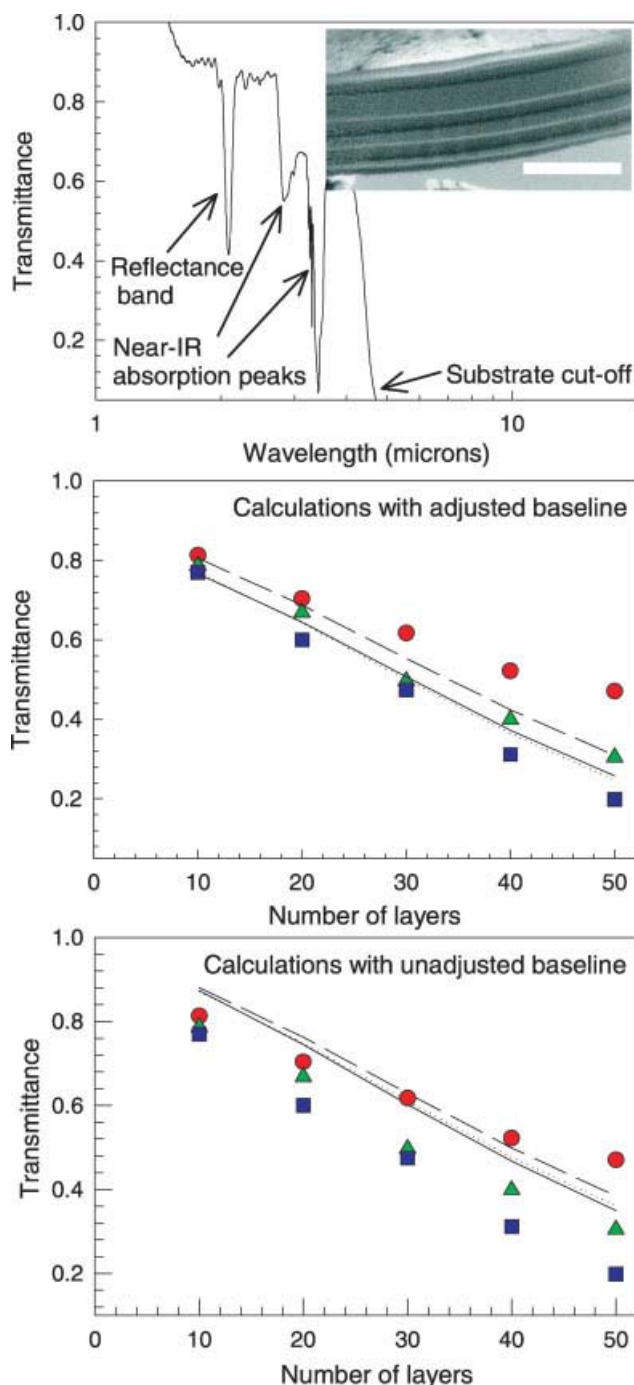


FIGURE 3 Wavelength and layer number dependence of the transmittance in PVP/PS multilayers. The top panel shows the transmittance of a 40 layer PVP/PS sample supported on a glass substrate which has $d_{PS} = 271$ nm and $d_{PVP} = 411$ nm. Data are shown for the 1–20 μm wavelength range. Features corresponding to the reflectance band, near IR absorption peaks in PS and PVP and the cut-off due to the glass substrate are clearly marked. The inset in this panel shows a SEM image of the top seven layers of a typical PS/PVP multilayer structure (scale bar: 2 μm). The bottom layer in the image is a PS film, the next is a PVP film and the sequence repeats. The bottom two panels show the minimum transmittance (1-peak reflectance) values in the near infrared region (1.6–2.7 μm) for multilayers as a function of the number of layers. Data are shown for multilayers with peaks at 1.738 ± 0.001 (red \circ), 2.224 ± 0.001 (green Δ), and 2.596 ± 0.001 μm (blue \square). The lines in the middle panel show the results of calculations where the baseline has been adjusted to include the effects of the additional glass-air interface present on the substrate. The bottom panel shows the same data as the middle panel with the results of calculations where this additional interface has not been taken into account. In both plots the dotted lines are calculations for the 2.596 μm peaks and the solid and dashed lines are the results of calculations for the 2.224 μm and 1.738 μm peaks, respectively.

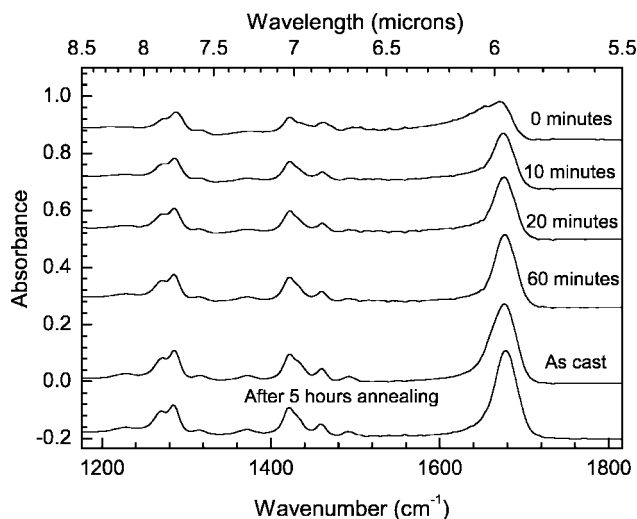


FIGURE 4 FTIR absorption spectra for PVP films on CaF_2 substrates. Data are shown for an as-cast film and spectra that were collected immediately (0 minutes), 10, 20, and 60 minutes after exposure to HCl vapor. An IR spectrum is also shown for a PVP film that was annealed at 110°C for 5 hours.

PS layer and before the deposition of the new PVP layers. This would seem to indicate that the PS layers are capable of protecting the underlying multilayer structure from the potentially disruptive influence of the acetonitrile/ethanol blends used to deposit new PVP layers. However, untreated PVP layers appear to allow the toluene that is used to deposit new PS layers to penetrate the multilayer structure and disrupt underlying PS layers.

Figure 4 shows FTIR spectra that were collected from PVP films both before and after exposure to the HCl vapor to determine what effects (if any) the swelling step has on the chemical properties of the films. The figure clearly shows that when the PVP films are exposed to the HCl vapor, there is a significant broadening of the polymer peaks. This is particularly true of the peak at 1720 cm^{-1} ($\sim 6\ \mu\text{m}$) corresponding to the stretching mode of the carbonyl groups in the polymer.²³ These changes in peak shape are indicative of the polar HCl molecules associating with the carbonyl groups in the side groups of the PVP. Such an association is likely to result in the carbonyl groups having a range of different local environments and will therefore result in a broadening of the corresponding vibrational peaks. When the samples are removed from the HCl vapor these peaks gradually relax back towards the shape of the as-cast PVP peaks when the samples are held at room temperature. The other vibrational peaks in the spectra corresponding to CH and possibly CN vibrations ($\sim 1380\text{ cm}^{-1}$ and $\sim 1100\text{ cm}^{-1}$) are largely unaffected by the HCl vapor. The spectra shown in Figure 4 indicate that the HCl has a relatively long dwell time (~ 1 hour) in the PVP films compared to the timescales that are associated with the deposition of successive layers during the automated spin coating process (~ 60 seconds).

These data and observations combined with the fact that it was not possible to produce high quality multilayers in the

absence of the HCl swelling step suggest that swelling the PVP films with HCl vapor prevents the diffusion of organic solvents such as toluene through the swollen PVP layers and hence prevents the subsequent disruption of underlying PS layers. Moreover, the fact that the PVP peaks relax back to shapes that are similar to those of unswollen samples indicates that no significant chemical changes (e.g., degradation or cross linking) are taking place in the polymer films. This conclusion is further supported by the fact that PVP films that have been swollen by HCl and then annealed have similar IR spectra to as-cast films. We note that there are some small differences in the shape of the spectra for the annealed and as-cast samples, but these are attributed to the removal of residual amounts of spin coating solvents that were present in the as-cast films. Films of PS of similar thickness that were treated using the same swelling conditions displayed no obvious spectral changes, indicating that HCl does not significantly affect the PS films. This is to be expected based upon the hydrophobic nature of this polymer.

CONCLUSIONS

We have demonstrated that it is possible to use spin coating to produce high quality dielectric mirrors with at least 50 alternating layers of PS and PVP that are capable of reflecting up to 80% of radiation over a narrow range of wavelengths in the $1.6\text{--}2.6\ \mu\text{m}$ region. The position and widths of the peaks observed are consistent with the results of predictions obtained from a consideration of simple multilayer interference and could be controlled by varying the spin speed used when depositing the individual layers. The measured transmittance spectra for these samples were also found to be in good agreement with the results of a simple transfer matrix model which assumes sharp interfaces between the individual layers. The properties of the multilayers produced were found to be highly dependent upon a HCl treatment step. This treatment step was shown to swell the PVP layers and appears to prevent diffusion of organic solvents into the underlying multilayer structure when new layers are deposited.

ACKNOWLEDGMENTS

The authors are grateful to Lloyd Hamilton (Centre for Biomolecular Sciences, University of Nottingham) for the OsO_4 staining of the polymer samples. They also thank Michael Fay and Chris Parmenter in the NNNC for collecting the SEM images.

REFERENCES AND NOTES

- Kimura, M.; Okahara, K.; Miyamoto, T. *J. Appl. Phys.* **1979**, *50*, 1222–1225.
- Adawi, A. M.; Connolly, L. G.; Whittaker, D. M.; Lidzey, D. G.; Smith, E.; Roberts, M.; Qureshi, F.; Foden, C.; Athanassopoulou, N. *J. Appl. Phys.* **2006**, *99*, 054505.
- Colodrero, S.; Mihi, A.; Haggman, L.; Ocana, M.; Boschloo, G.; Hagfeldt, A.; Miguez, H. *Adv. Mater.* **2009**, *21*, 764–770.
- Takeuchi, H.; Natsume, K.; Suzuki, S.; Sakat, H. *Elec. Lett.* **2007**, *43*, 30–31.

- 5 Yoon, J.; Lee, W.; Thomas, E. L. *Nano Lett.* **2006**, *6*, 2211–2214.
- 6 Yoon, J.; Lee, W.; Caruge, J.-M.; Bawendi, M.; Thomas, E. L.; Kooi, S.; Prasad P. N. *Appl. Phys. Lett.* **2006**, *88*, 091102.
- 7 Singer, K. D.; Kazmierczak, T.; Lott, J.; Song, H.; Wu, Y.; Andrews, J.; Baer, E.; Hiltner, A.; Weder, C. *Opt. Express* **2008**, *16*, 10358–10363.
- 8 Komikado, T.; Yoshida, S.; Umegaki, S. *Appl. Phys. Lett.* **2006**, *89*, 061123.
- 9 Komikado, T.; Inoue, A.; Masuda, K.; Ando, T.; Umegaki, S. *Thin Solid Films* **2007**, *515*, 3887–3892.
- 10 Kinoshita, S.; Yoshioka, S.; Miyazaki, J. *Rep. Prog. Phys.* **2008**, *71*, 076401.
- 11 Adawi, A. M.; Cadby, A.; Connolly, L. G.; Hung, W.-C.; Dean, R.; Tahraoui, A.; Fox, A. M.; Cullis, A. G.; Sanvitto, D.; Skolnick, M. S.; Lidzey, D. G. *Adv. Mater.* **2006**, *18*, 742–747.
- 12 Bailey, J.; Sharp, J. S. *Eur. Phys. J. E.* **2010**, *33*, 41–49.
- 13 Brandrup, J.; Immergut, E. H.; Grulke, E. A. *Polymer Handbook*; Wiley: New Jersey, 1999.
- 14 Alvarez, A. L.; Tito, J.; Vaello, M. B.; Velasquez, P.; Mallavia, R.; Sanchez-Lopez, M. M.; Fernandez de Avila, S. *Thin Solid Films* **2003**, *433*, 277–280.
- 15 Kohoutek, T.; Orava, J.; Hrdlicka, M.; Wagner, T.; Vlcek, M.; Frumar, M. *J. Phys. Chem. Solids* **2007**, *68*, 2376–2380.
- 16 DeCorby, R. G.; Nguyen, H. T.; Dwivedi, P. K.; Clement, T. J. *Optics Express* **2005**, *13*, 6228–6233.
- 17 Ho, P. K.; Thomas, D. S.; Friend, R. H.; Tessler, N. *Science* **1999**, *285*, 233–236.
- 18 Walker, P. M.; Sharp, J. S.; Akimov, A. V.; Kent, A. J. *Appl. Phys. Lett.* **2010**, *97*, 073106.
- 19 Hecht, E. *Optics*, 2nd ed.; Addison-Wesley: Amsterdam, 1987.
- 20 Katsidis, C. C.; Siapkis, D. I. *Appl. Opt.* **2002**, *41*, 3978–3987.
- 21 Azzam, R. M. A.; Bashara, N. M. *Ellipsometry and Polarized light*; Elsevier: London, 1987.
- 22 Ennis, D.; Betz, H.; Ade, H. *J. Polym. Sci. Part B: Polym. Phys.* **2006**, *44*, 3234–3244.
- 23 Oster, G.; Immergut, E. H. *J. Am. Chem. Soc.* **1954**, *76*, 1393–1396.